

THE ULTRAVIOLET SPECTRA OF LINERs: A COMPARATIVE STUDY¹

DAN MAOZ,² ANURADHA KORATKAR,³ JOSEPH C. SHIELDS,⁴ LUIS C. HO,⁵ ALEXEI V. FILIPPENKO,⁶ AND AMIEL STERNBERG^{2,6}

Received 1997 October 27; revised 1998 April 1

ABSTRACT

Imaging studies have shown that $\sim 25\%$ of LINER galaxies display a compact nuclear UV source. As part of a program to study the nature of LINERs and their connection to the active galaxy phenomenon, we compare the *Hubble Space Telescope* UV (1150–3200 Å) spectra of seven such UV-bright LINERs. Data for three of the galaxies (NGC 404, 4569, and 5055) are presented for the first time, while data for four others (M81, NGC 4594, NGC 4579, and NGC 6500) have been recently published. The spectra of NGC 404, 4569, and 5055 show clear absorption-line signatures of massive stars, indicating a stellar origin for the UV continuum. Similar features are probably present in NGC 6500. The same stellar signatures may be present but undetectable in NGC 4594, because of the low signal-to-noise ratio of the spectrum, and in M81 and NGC 4579, because of superposed strong, broad emission lines. The compact central UV continuum source that is observed in these galaxies is a nuclear star cluster rather than a low-luminosity active galactic nucleus (AGN), at least in some cases. Except for the two LINERs with broad emission lines (M81 and NGC 4579), the LINERs have weak or no detectable UV emission lines. The UV emission-line spectrum strength shows no relation to the UV continuum strength. Furthermore, at least four of the LINERs suffer from an ionizing photon deficit in the sense that the ionizing photon flux inferred from the observed far-UV continuum is insufficient to drive the optical H I recombination lines. Examination of the nuclear X-ray flux of each galaxy shows a high X-ray-to-UV ratio in the four “UV photon-starved” LINERs. In these four objects, a separate component, emitting predominantly in the extreme-UV, is the likely ionizing agent and is perhaps unrelated to the observed nuclear UV emission. Future observations can determine whether the UV continuum in LINERs is always dominated by a starburst or, alternatively, that there are two types of UV-bright LINERs: starburst dominated and AGN dominated.

Key words: galaxies: active — galaxies: nuclei — galaxies: star clusters — ultraviolet emission

1. INTRODUCTION

Low-ionization nuclear emission-line regions (LINERs) are detected in the nuclei of a large fraction of all bright nearby galaxies (Ho, Filippenko, & Sargent 1997a). Since their definition as a class by Heckman (1980), they have elicited debate as to their nature and relation, if any, to active galactic nuclei (AGNs). On the one hand, the luminosities of most LINERs are unimpressive compared with “classical” AGNs and can easily be produced by processes other than accretion onto massive black holes. Indeed, LINER-like spectra are sometimes seen to arise in “nonnuclear” environments, such as cooling flows. On the other hand, a variety of observables point to similarities and continuities between AGNs and, at least, some LINERs (for reviews, see the contributions in Eracleous et al. 1996). If LINERs represent the low-luminosity end of the AGN phe-

nomenon, then they are the nearest and most common examples and their study is germane to understanding AGN demographics, quasar evolution, dormant black holes in quiescent galaxies, the X-ray background, and the connection between AGN-like and starburst-like activity.

The ultraviolet sensitivity and angular resolution of the *Hubble Space Telescope* (*HST*) are providing new clues toward understanding LINERs. Maoz et al. (1996a) carried out a UV (2300 Å) imaging survey of the central regions of 110 nearby galaxies with the Faint Object Camera (FOC) on *HST*. As reported in Maoz et al. (1995), five among the 25 LINERs in their sample revealed nuclear UV sources, in most cases unresolved, implying physical sizes $\lesssim 2$ pc. Maoz et al. (1995) argued that the UV sources in these “UV-bright” LINERs could be the extension of the ionizing continuum, which is rarely seen in LINERs at optical wavelengths because of the strong background from the normal bulge population. The compactness of the sources suggested that they could be nonstellar in nature, although compact star clusters of such luminosity were also possible. A similar fraction of UV-bright nuclei was found in a 2200 Å imaging survey of 20 LINER and low-luminosity Seyfert 2 galaxies carried out with the Wide Field Planetary Camera 2 (WFPC2) on *HST* by Barth et al. (1996a, 1998). A compact, isolated, nuclear UV source has also been found in FOC images of the LINER NGC 4594 at ~ 3400 Å by Crane et al. (1993) and in WFPC2 images of the LINER M81 in a broad (1100 to 2100 Å) bandpass by Devereux, Ford, & Jacoby (1997). The UV-bright LINERs were obvious targets for follow-up spectroscopy with *HST*. Faint Object Spectrograph (FOS) observations have been analyzed for the LINERs M81 (Ho, Filippenko, & Sargent

¹ Based on observations with the NASA/ESA *Hubble Space Telescope*, obtained at the Space Telescope Science Institute, which is operated by the Association of Universities for Research in Astronomy, Inc., under NASA contract NAS 5-26555.

² School of Physics and Astronomy and Wise Observatory, Tel Aviv University, Ramat Aviv, Tel Aviv 69978, Israel; dani@wise.tau.ac.il, amiel@wise.tau.ac.il.

³ Space Telescope Science Institute, 3700 San Martin Drive, Baltimore, MD 21218; koratkar@stsci.edu.

⁴ Department of Physics and Astronomy, Ohio University, Clippingier Labs 251B, Athens, OH 45701; shields@helios.phy.ohiou.edu.

⁵ Harvard-Smithsonian Center for Astrophysics, 60 Garden Street, Cambridge, MA 02138; lho@coyote.harvard.edu.

⁶ Department of Astronomy, University of California at Berkeley, 601 Cambell Hall, Berkeley, CA 94720-3411; alex@astro.berkeley.edu.

1996), NGC 4579 (Barth et al. 1996b), NGC 6500 (Barth et al. 1997), and NGC 4594 (Nicholson et al. 1998). Among these four, NGC 4579 was part of the Maoz et al. (1995) FOC survey and NGC 6500 was in the Barth et al. (1996a, 1998) WFPC2 survey.

The spectra of M81 and NGC 4579, which in the optical range have weak broad wings in the H α line (Filippenko & Sargent 1985, 1988; Ho et al. 1997b), are reminiscent of AGNs in the UV, with strong broad emission lines superposed on a featureless continuum. Ho et al. (1996) and Barth et al. (1996b) concluded that these two LINERs are most probably AGNs. NGC 6500 and NGC 4594, on the other hand, have only weak and narrow emission lines on top of a UV continuum. Based on the resolved appearance of the UV source in the *HST* WFPC2 F218W image and the tentative detection of optical Wolf-Rayet features, Barth et al. (1997) concluded that the UV emission in NGC 6500 is likely dominated by massive stars, though contribution from a scattered AGN component could not be excluded. For NGC 4594, Nicholson et al. (1998) favor an AGN interpretation.

In this paper, we present FOS UV spectra of three additional LINERs (NGC 404, 4569, and 5055) and compare the properties of all seven UV-bright LINERs observed spectroscopically to date with *HST*.

2. OBSERVATIONS

The three LINERs with new data were observed with a similar observational setup to that used for the four previously published LINERs. The FOS 0".86 diameter circular aperture was centered on the nucleus using a three-stage peak-up, and three grating/detector combinations were used: G130H/FOS-BLUE (1152–1608 Å, 1.0 Å diode⁻¹), G190H/FOS-RED (1600–2280 Å, 1.5 Å diode⁻¹), and G270H/FOS-RED (2222–3277 Å, 1.0 Å diode⁻¹). The spectral resolution is about half a diode. Table 1 lists the main observational parameters for the seven objects. Among the previously studied LINERs, M81 and NGC 4579 were observed with the 0".3 and 0".43 diameter apertures, respectively. This should make little difference compared with the 0".86 apertures used for the other objects, since Maoz et al. (1995) demonstrated that the main central UV source in NGC 4579 has FWHM < 0".11, and Devereux et al. (1997) found that the UV source in M81 has FWHM < 0".1. Similarly, the UV images of most of the objects (Maoz et al.

1995; Barth et al. 1996a, 1998; Devereux et al. 1997) show that all the UV flux from the central compact UV source would be included in the FOS aperture, and light from neighboring sources excluded. This statement holds with less confidence for NGC 4594, where UV imaging data exist only in the near-UV (3400 Å; Crane et al. 1993), but the nucleus appears unresolved and isolated at that wavelength.

The spectra of the three LINERs with new data were reduced, as in the case of the previously studied objects, by the standard *HST* calibration pipeline, which includes flat-fielding, subtraction of the particle-induced background, and flux and wavelength calibration. We reiterate the conclusions of Barth et al. (1997) and Nicholson et al. (1998) that in the two faintest objects, NGC 6500 and NGC 4594, the correction for scattered light toward short wavelengths in the G130H grating is only approximate. In NGC 4594, the G130H flux is dominated by scattered light, so the continuum shape measured in that spectral region is unreliable.

Table 1 also gives a comparison of the observed ~ 2200 Å flux density measured from the FOS spectra with the flux from *HST* broadband measurements at that wavelength. Such a comparison is relevant for appraising the accuracy of the spectroscopic measurements and looking for evidence of variability. For M81, we have used the FOS spectra and the WFPC2 F160BW throughput curve to derive the 1500 Å continuum flux that would produce the count rate observed in the WFPC2 image of Devereux et al. (1997). Note that the level of agreement between the various measurements of the same object is mixed. The uncertainty of the FOC F220W measurements of individual sources is $\sim 20\%$, because of flat-fielding and background uncertainties (Meurer et al. 1995). The uncertainty is larger for sources that Maoz et al. (1995) could not fit properly with the pre-COSTAR *HST* point-spread function because of additional diffuse and compact sources near the main central UV source (e.g., in NGC 404 and NGC 5055). For M81, the variable sensitivity of WFPC2 in the far-UV and the unknown spectrum of the object in the G190H range both contribute to the uncertainty. From an analysis of the FOS target acquisition records, we deduce that NGC 404 and M81 were found at the edges of the peak-up scans, possibly compromising the photometric accuracy of their observations. In view of all this, the FOC, WFPC2, and FOS measurements of a given object in Table 1 are consistent, except for the case of NGC 4579.

TABLE 1
OBSERVATION JOURNAL

GALAXY	v_h (km s ⁻¹)	DATE (UT)	APERTURE (arcsec)	EXPOSURE TIME (s)			OBSERVED $f_\lambda(2200 \text{ Å})^a$			GALACTIC $E(B-V)$
				G130H	G190H	G270H	FOS	FOC ^b	WFPC2 ^c	
NGC 404	-36	1994 Dec 25	0.86	6400	2130	540	115	180	...	0.055 ^d
M81	-28	1993 Apr 5, 14	0.30	3000	...	2000	150 ^e	...	200 ^e	0.035 ^d
NGC 4569	-223	1996 Apr 11	0.86	4790	1320	690	1050	1000	1100	0.050 ^f
NGC 4579	1500	1994 Dec 16	0.43	6840	3300	690	33	110	...	0.052 ^f
NGC 4594	1128	1995 Jan 12	0.86	3720	1800	480	12	0.066 ^f
NGC 5055	497	1996 Apr 12	0.86	7380	2510	2440	77	100	...	0.000 ^d
NGC 6500	3003	1994 Aug 13	0.86	10260	3110	1020	27	...	27	0.093 ^d

^a In units of 10^{-17} ergs s⁻¹ cm⁻² Å⁻¹.

^b Maoz et al. 1995.

^c Barth et al. 1998.

^d Burstein & Heiles 1984.

^e At 1500 Å rather than 2200 Å and computed from the WFPC2 counts by assuming a scaled version of the 1600–2300 Å spectrum of NGC 4579.

^f From Murphy et al. 1996.

As discussed by Barth et al. (1996b), in NGC 4579 the FOS 2200 Å flux is less than one third that implied by the FOC measurement made 19 months earlier. Barth et al. (1996b) interpreted the difference as due to variability of a nonstellar continuum source. However, there is a chance that the low FOS flux was the result of a miscentered aperture. We note that there is a second, slightly extended UV source 0".58 east of the main nuclear source, which has about one-sixth of its flux (see Maoz et al. 1995). The FOS 0".43 aperture may have been accidentally centered between this source (which might be relatively brighter in the G270H grating's wavelength range, in which the peak-up procedure was done) and the central source, bringing the edge of the aperture, say, 0".1 from the central source. Half of the flux in the observed spectrum would then be from the secondary source and half from the fraction of the point-spread function of the central source within the aperture. We have reanalyzed the *HST* records of the target acquisition for this observation, and they indicate that the FOS aperture was properly centered on the brighter of two sources, if two were present. Furthermore, a broadband visual (F547M) WFPC2 exposure of the galaxy (to be described elsewhere) shows a single unresolved nucleus, with no trace of an additional source to the east. This supports the variability interpretation. It would be valuable, however, to confirm such variability in this and other LINERs.

We also list in Table 1 the Galactic reddening, $E(B-V)$, that we have adopted for each object, based on the H I column density N_H from Murphy et al. (1996) if available,

with the conversion $E(B-V) = N_H / (5.8 \times 10^{21} \text{ cm}^{-2})$ or using Burstein & Heiles (1984). For NGC 6500, we have followed Barth et al. (1996b) and used the Burstein & Heiles (1984) value, despite the availability of a measurement by Murphy et al. (1996). Correcting the NGC 6500 spectrum using the Murphy et al. (1996) value leads to a distinct bump in the continuum at 2200 Å.

Figures 1–4 below show sections of the spectra of the seven LINERs. We analyze and compare them below.

3. ANALYSIS

3.1. Far-UV Spectral Signatures of Massive Stars

Figure 1 shows most of the G130H spectrum of all seven LINERs (the extreme red and blue ends are excluded). The objects are ordered with the two broad-lined LINERs (M81 and NGC 4579) on top and the other LINERs in order of decreasing f_λ . Figure 2 shows in more detail the same spectral region for NGC 4569, 404, 5055, and 6500. Here and in the following figures, all the spectra have been shifted to the object's rest frame (according to the velocities listed in Table 1) and binned into 1 or 2 Å bins to improve the signal-to-noise ratio (S/N). Overlaid on each spectrum (*light line*) is a scaled, normalized version of the *HST* Goddard High Resolution Spectrograph spectrum of the "B" clump in NGC 1741, a starburst galaxy, which is described by Conti, Leitherer, & Vacca (1996). The broad blueshifted absorption profiles of C IV $\lambda 1549$ and Si IV $\lambda 1400$ (and also N V $\lambda 1240$) in NGC 1741B are the signatures of winds

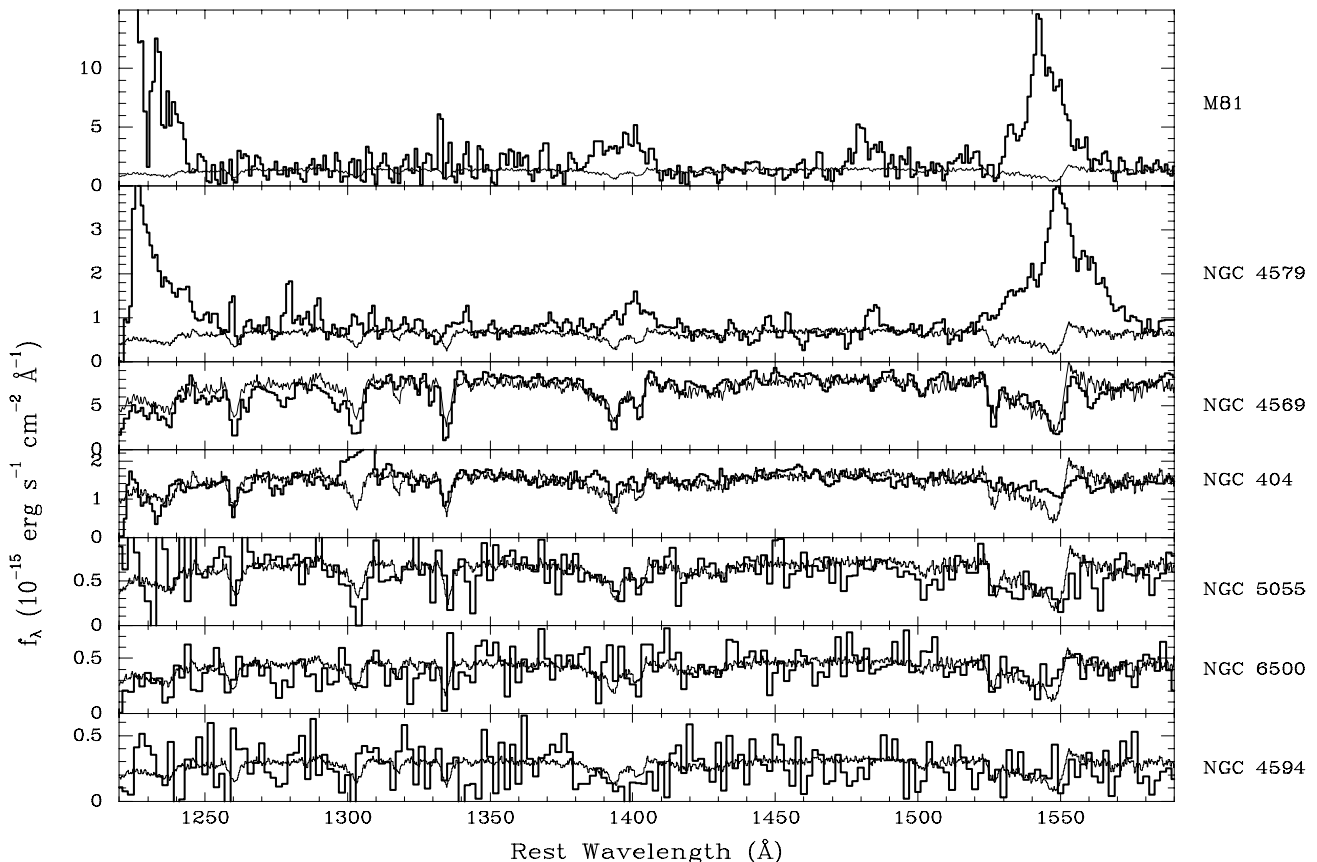


FIG. 1.—FOS G130H spectra of the seven LINERs (*heavy lines*) ordered with the two broad-lined objects on top and then with decreasing f_λ . Overlaid in each case is the spectrum of the starburst in NGC 1741B normalized to be flat in f_λ and scaled by a multiplicative factor to match the LINER continuum level.

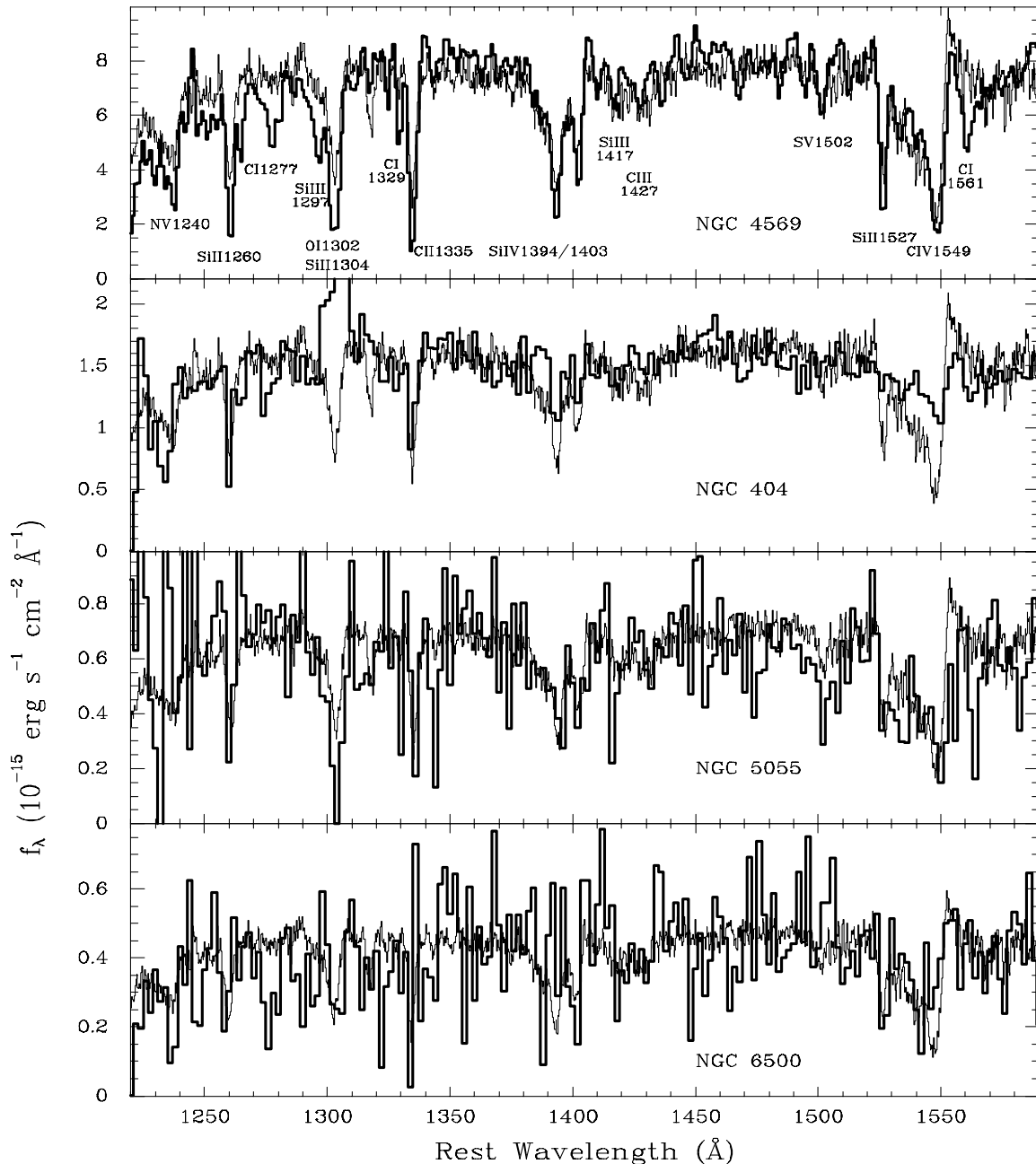


FIG. 2.—Same as Fig. 1, but for only the four brightest LINERs devoid of broad emission lines. The strongest absorption lines are labeled for NGC 4569. The emission feature near 1300 Å in NGC 404 is an artifact.

produced by massive stars (see Leitherer, Robert, & Heckman 1995). The other, narrower, absorption lines are of both photospheric and interstellar medium (ISM) origin. The characteristic starburst features seen in the spectrum of NGC 1741B are also observed in star-forming regions in 30 Doradus (Vacca et al. 1995) and NGC 4214 (Leitherer et al. 1996), in star-forming galaxies at redshifts $z \approx 2-3$ (Steidel et al. 1996; Lowenthal et al. 1997), and in the $z = 3.8$ starburst radio galaxy 4C 41.17 (Dey et al. 1997).

The FOS spectrum of NGC 4569, the brightest (and highest S/N) LINER in our sample, is virtually identical to that of NGC 1741B. Most of the features in the two spectra match one-to-one. NGC 4569 has all the main interstellar

absorption lines seen in starburst spectra, as well as the broad stellar wind features. Also detected are several narrow absorption lines that cannot be interstellar (they are not resonance lines) and constitute further evidence of the photospheres of hot stars: Si III $\lambda 1294/\lambda 1297$, Si III $\lambda 1417$, C III $\lambda 1427$, S V $\lambda 1502$, and N IV $\lambda 1720$ (Heckman & Leitherer 1997). The correspondence between the two spectra is such that a dilution of the stellar features by a nonstellar (i.e., featureless) continuum producing more than 20% of the UV continuum would be readily apparent. The only significant difference between the spectra of the starburst clump in NGC 1741 and the nucleus of NGC 4569 is the presence of relatively strong C I absorption lines (at rest

TABLE 2
ABSORPTION-LINE EQUIVALENT WIDTHS

Line	NGC 4569	NGC 404	NGC 5055	Milky Way
N v $\lambda 1240^a$	2.8	3.5
Si II $\lambda 1260$	2.6	1.7	1.8	0.6–1.4
C I $\lambda 1261$	1.0 ^b
C I $\lambda 1277$	1.4	0.7
C I $\lambda 1280$	0.6
Si III $\lambda \lambda 1294, 1297^c$	0.8
O I $\lambda 1302$ + Si II $\lambda 1304$	4.2	...	4.0	0.8–1.7
C I $\lambda 1329$	1.2
C II $\lambda 1335$	3.6	2.0	...	0.8–1.0
Si IV $\lambda \lambda 1394, 1403^a$	8.3	2.9	7.8	0.8
Si III $\lambda 1417^c$	0.5
C III $\lambda 1427^c$	0.4
S V $\lambda 1502^c$	1.3
Si II $\lambda 1527$	2.3	...	1.6	0.5–0.7
C IV $\lambda 1549^a$	11	4.8	15	0.3–0.5
C I $\lambda 1561$	1.2 ^d	0.8
Fe II $\lambda 1608$	1.5 ^e
C I $\lambda 1657$	3.6
Al II $\lambda 1670$	3.5	2.5	2.1	0.6–0.8
N IV $\lambda 1720^c$	1.6
Fe II $\lambda 2344$	2.9 ^e	2.2	2.1	0.7–1.2
Fe II $\lambda 2374$	2.1 ^e	1.2	...	0.6–1.0
Fe II $\lambda 2383$	3.4 ^e	1.4	3.2	0.8–1.4
Fe II $\lambda 2586$	2.4 ^e	1.8	2.0	0.6–1.1
Fe II $\lambda 2600$	3.3 ^e	2.5	2.6	0.9–1.5
Mg II $\lambda 2800$	9.9	7.5	9.6	2.1–3.4
Mg I $\lambda 2852$	1.8	1.7	2.7	0.4–0.6

NOTES.—Equivalent widths in angstroms. The Milky Way range is based on quasar spectra from Savage et al. 1993.

^a Interstellar, plus broad blueshifted absorption from O-type star atmospheres.

^b After approximate deblending from Si II $\lambda 1260$.

^c Nonresonance line originating in the photospheres of hot stars.

^d Difficult to determine the continuum level because of C IV $\lambda 1549$ absorption.

^e From the line profile, roughly one-fourth of the absorption is Galactic.

wavelengths 1277, 1280, 1329, 1561, and 1657 Å) in NGC 4569.⁷ All the absorption lines are at the slight blueshift (-223 km s^{-1}) of the galaxy and hence are not produced in the ISM of the Milky Way. Table 2 lists the main absorption lines detected. There is no doubt that the UV emission in this object, even though its source is highly compact ($\lesssim 2 \text{ pc}$; Maoz et al. 1995), is dominated by a cluster of massive stars. Keel (1996) reached a similar conclusion regarding the optical continuum emission, based on the presence of narrow Balmer line absorption, characteristic of A-type supergiants. The luminosity of a star cluster is dominated by the most massive stars. Using spectral synthesis models (see § 3.3) and assuming a distance of 9 Mpc (Rood & Williams 1993) to this galaxy, we estimate that 250–600 O-type stars (depending on the presence of very massive early O-type stars) are sufficient to produce the observed luminosity (in our models, O-type stars are defined as stars having temperatures $T \geq 30,900 \text{ K}$). As discussed in more detail in § 3.2 below, a plausible amount of dust extinction can raise this number by factors of up to several tens.

Proceeding to the far-UV spectrum of NGC 404 (Fig. 2), we note that the broad, blueshifted C IV absorption is shal-

lower but definitely detected. Si IV absorption is not seen, except in the narrow components. According to the synthesis by Leitherer et al. (1995), such spectra characterize a starburst that is either very young ($< 3 \text{ Myr}$) or older than 5 Myr. The denser winds of O-type supergiants, which are present only during a limited time, are required in order to produce the broad blueshifted Si IV absorption. The C IV absorption, on the other hand, remains as long as there are main-sequence O-type stars. The relative shallowness of the C IV profile can also be reproduced well by diluting the NGC 1741B starburst spectrum with a featureless (e.g., nonstellar) spectrum that is constant in f_λ and contributes $\sim 60\%$ of the total flux. The strongest interstellar absorption lines that appear in NGC 4569, including the C I lines, are seen in NGC 404 as well. Because of the small blueshift of this galaxy (-36 km s^{-1}), we cannot say whether these lines arise in the Milky Way or in NGC 404 based on their wavelengths alone. However, *HST* studies of Milky Way absorption along the lines of sight to quasars (Savage et al. 1993) show that the equivalent widths of Milky Way absorption in these transitions are several times smaller than the equivalent widths listed for the LINERs in Table 2. For the sake of comparison, we include in Table 2 the range of Galactic equivalent widths measured by Savage et al. (1993). The velocity width and blueshift of the C IV profile clearly point to a stellar origin for this line. (The “emission” between 1295 and 1310 Å in NGC 404 is an artifact due to a noisy diode that masks the O I and S II absorptions that are probably present at those wavelengths.) It thus appears that the UV continuum source in this LINER is a star cluster

⁷ The C I lines are generally not seen with such strength (up to 3.5 Å equivalent width) in starburst spectra. It is of interest that the same C I lines seem to be present in some of the other LINERs as well, so they may be a signature of a particular sort of environment. We discuss the interstellar lines in more detail in the Appendix.

that is of different age than the one in NGC 4569 or, perhaps, a cluster of similar age whose emission is diluted by a nonstellar continuum. Assuming a distance of 2 Mpc (Tully 1988) to NGC 404, its UV luminosity is 100 times lower than that of NGC 4569, implying that just two to six O-type stars can produce the observed luminosity. Again, the actual number is likely higher after a reasonable extinction correction.

Continuing to the G130H spectrum of NGC 5055 (Fig. 2), the S/N degrades, but the blueshifted broad C iv and Si iv absorptions seen in NGC 4569 are definitely present. Their minima are at the galaxy's redshift (497 km s^{-1}). The properly redshifted minimum, the width, and the blue asymmetry of the C iv profile all argue against the possibility that we are merely seeing a blend of strong Milky Way or host galaxy ISM absorption lines. The absorption lines may be slightly broader than in NGC 4569. From the G270H spectrum, which has a higher S/N, we also find that the dominant ISM absorptions are in the host galaxy, not the Milky Way. The stellar nature of this UV source is not surprising, since Maoz et al. (1995) already noted that it is marginally resolved at 2200 \AA , with $\text{FWHM} \approx 0''.2$ ($\approx 6 \text{ pc}$). NGC 4569 and NGC 5055 are remarkably similar over the entire UV range. Overall, the spectrum of NGC 5055 resembles a lower S/N version of that of NGC 4569. At a distance of 6 Mpc (Phillips 1993), NGC 5055 is ~ 20 times less luminous than is NGC 4569.

In the spectrum of NGC 6500 (Fig. 2), the blueshifted broad C iv absorption is possibly recognizable, although as noted by Barth et al. (1997), its significance is arguable when the spectrum is viewed individually. The comparison with the spectra of the other LINERs and the starburst spectrum, combined with the obvious degradation in S/N in this fainter object, suggest that the absorption may, in fact, be present. The spectrum is too noisy and dominated by scattered light to reach any conclusion regarding the Si iv absorption. As noted above, Barth et al. (1997) already concluded, based on the extended ($0''.5 \approx 100 \text{ pc}$) appearance of the UV source in a WFPC2 image, that this source is probably stellar in nature.

Finally, the NGC 4594 G130H data (Fig. 1) are too noisy and dominated by scattered light to reach any conclusion except that they could be consistent with the same type of spectrum. There are certainly no strong *emission* lines in this part of the spectrum of NGC 4594.

We conclude that, in the five LINERs without emission lines in the G130H range, the UV continuum is, with varying degrees of certainty, produced by massive young stars. Could the same be true of the two broad-lined LINERs in our sample, M81 and NGC 4579? As already noted by Ho et al. (1996) for M81, one cannot answer this question based on these UV data alone. Figure 1 shows that if the continuum spectrum were of the same starburst type as in the other LINERs we would not know it, because the broad emission lines are coincident with the broad absorptions. A case in point is the recent study by Heckman et al. (1997) of the Seyfert 2 galaxy Mrk 477. The relatively narrow emission lines are superposed on the broad stellar wind signatures, but in Si iv and N v enough of the stellar absorptions are visible near the blue wings of the emission lines to reveal the starburst nature of the UV continuum emission. In M81 and NGC 4579, however, the emission lines are too broad to see the stellar absorptions, if they are there.

One may alternatively hope to detect the narrow interstellar absorption lines that also typify starburst spectra (or to put upper limits on the presence of such lines). We see, however, that even in NGC 4579, which has a higher S/N G130H spectrum than does M81, the interstellar lines would not be detected even if they were present. Indeed, in the regions between the broad emission lines, the scaled starburst spectrum appears more "featureless" than the continuum of NGC 4579. An S/N of about 20 in the continuum, as in NGC 4569, rather than about 5, as is the case in NGC 4579, would allow the detection of interstellar lines in the spectrum. The single argument that the UV continuum source in NGC 4579 is necessarily nonstellar is based on its possible factor of ~ 3 variability reported in Barth et al. (1996b).

The compact UV continuum sources in three or four of the seven LINERs are therefore clusters with massive stars. Barring perhaps NGC 4579 (assuming its UV variability is real), the UV continuum in *all* the LINERs could be stellar in origin. Note that this result does not bear directly on the question of whether or not there is also a nonstellar, quasar-like object in the nucleus. A microquasar could still be present and dominate the emission at wavelengths other than the UV. Indeed, we will show below that additional continuum energy, beyond what is implied by the stellar UV continuum, is required by the emission-line energy budget in some of these LINERs. Furthermore, it is becoming increasingly appreciated that circumnuclear starbursts, albeit on physical scales larger than those considered here, can contribute significantly to the UV and optical brightness of some AGNs (e.g., IC 5135, Shields & Filippenko 1990; Heckman 1998; NGC 1068, Thatte et al. 1997; NGC 7469, Genzel et al. 1995; Mrk 477, Heckman et al. 1997; some Seyfert 2's, Heckman 1998).

3.2. UV Spectral Energy Distribution and Extinction

Figure 3 shows the UV spectral energy distributions (SEDs) of the seven LINERs as $\log f_\lambda$ versus $\log \lambda$ and in the same order as in Figure 1. The spectra have been corrected for Galactic extinction using the extinction curve of Cardelli, Clayton, & Mathis (1989), assuming $A_V = 3.1E(B-V)$ and the $E(B-V)$ values listed in Table 1. The spectra have been vertically shifted as indicated on the right-hand side, for clarity. The G130H spectrum of NGC 4594 is not plotted, because it is dominated by scattered light and, hence, unreliable. The straight lines drawn through every spectrum at $\log \lambda = 3.36$ (2300 \AA) are power laws $f_\lambda \propto \lambda^\beta$, with $\beta = 0, -1$, and -2 . The figure shows that the seven LINERs have UV SEDs that are similar. After the correction for Galactic reddening, most can be roughly described shortward of 2300 \AA by power laws with $\beta \approx -0.5$ to 0.5 . Table 3 lists β for the seven galaxies. NGC 4579 is again somewhat exceptional in that its slope changes shortward of 1900 \AA from $\beta \approx 0$ to $\beta \approx -1.5$ (Barth et al. 1996b). Typical Seyfert 1 AGNs have power-law continua with β of -1 to -1.5 in the UV. The intrinsic spectra of unreddened massive stars, and hence of synthesized young starbursts, rise even more steeply to the far UV, with $\beta \approx -2$ to -2.5 (Leitherer & Heckman 1995). Many observed starbursts also have similar slopes (Kinney et al. 1996), though not quite as steep as $\beta = -2.5$, even when their Balmer decrements indicate no reddening. An empirical starburst template spectrum derived by Calzetti (1997a) has $\beta = -2.1$. If the similarity of the LINER SEDs is the

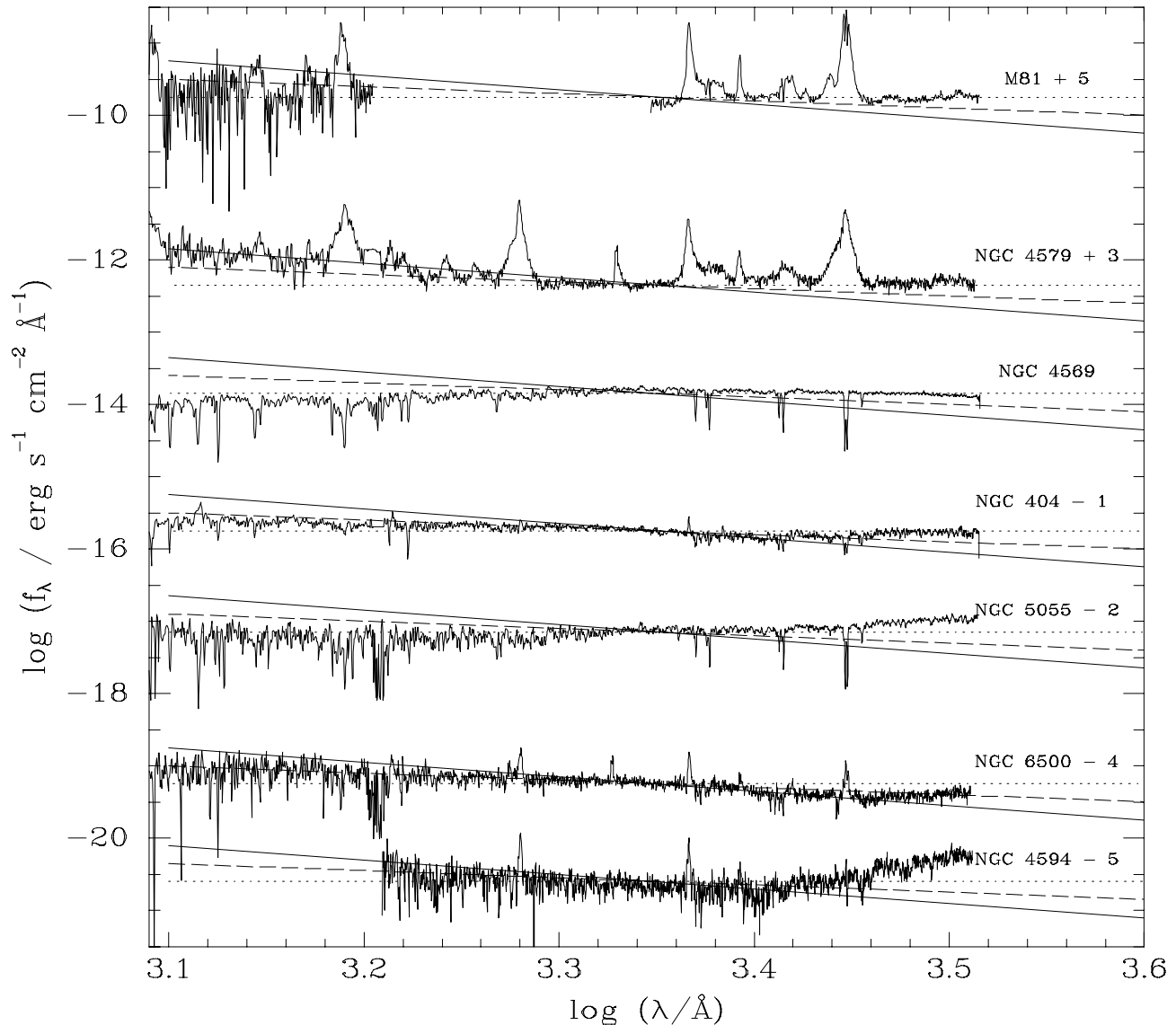


FIG. 3.—UV (1250–3200 Å) spectral energy distributions for the seven LINERs plotted as $\log f_\lambda$ vs. $\log \lambda$. The spectra have been corrected for Galactic extinction assuming the $E(B - V)$ values listed in Table 1 and vertically shifted for clarity as indicated on the right-hand side. The lines drawn through each spectrum at $\log \lambda = 3.36$ (2300 Å) are power laws $f_\lambda \propto \lambda^\beta$, with $\beta = 0, -1$, and -2 . The seven LINERs have similar UV spectral slopes. Excluding NGC 4579, they can be roughly described shortward of 2300 Å by power laws with $\beta \approx 0 \pm 0.5$.

result of reddening, it is puzzling that the reddening is generally tuned to produce a flat spectrum in f_λ , i.e., a change in slope between the intrinsic and the reddened spectrum of $\Delta\beta \approx 2$. The extinction law must be different from the Galactic one in order not to introduce a strong 2200 Å feature. A similar conclusion has been found to hold generally for starbursts by Calzetti, Kinney, & Storchi-Bergmann (1994, 1996).

UV extinction curves vary greatly depending on the environment and the geometry of sources, dust, and gas. To gauge the amount of extinction suffered by the UV sources in the LINERs, we first estimate the extinction from the slope β of the UV continuum. A change in slope $\Delta\beta$ corresponds to a reddening in magnitudes

$$A(1300 \text{ Å}) - A(2300 \text{ Å}) = 2.5\Delta\beta \log(2300/1300).$$

The translation of reddening to UV extinction depends on the assumed extinction curve. Following Pettini et al. (1998), we take two extreme possibilities of extinction curves

devoid of a 2200 Å bump. One is the steep extinction curve found for stars in the Small Magellanic Cloud (SMC) by Bouchet et al. (1985), as normalized by Pei (1992). The other is the “attenuation curve” empirically derived by Calzetti et al. (1994) from the spectra of star-forming galaxies, as normalized in Calzetti (1997b). The latter is “grayer” than the former, so it will produce more UV extinction for a given amount of reddening. For the SMC curve, $\Delta\beta = 2$ corresponds to $A_V = 0.4$ mag and $A_{1300} = 2.4$ mag. For the Calzetti et al. (1994) curve, one obtains $A_V = 1.9$ mag and $A_{1300} = 4.8$ mag. A plausible range for the attenuation factor at 1300 Å is therefore 10–80, at least for the “clearly stellar” LINERs, where we can be fairly confident about the intrinsic, unreddened spectral slope.

An independent estimate of the UV extinction in these objects can be obtained from their Balmer decrements. The decrements, as measured by Ho et al. (1997a), are listed in Table 3. The $H\alpha/H\beta$ ratio in NGC 4579, 5055, and 4569 is in the range 5–5.4. Assuming the steep SMC curve, this

TABLE 3
OBSERVED EMISSION

EMISSION	M81	NGC					
		4579	6500	4594	404	5055	4569
C iv $\lambda 1549$	140	70.0	<1.0	<1.6	<2.0	<2.0	<2.0
He II $\lambda 1640$	5.8	1.9	<1.4	3.5	<2.0	<2.0
C III] $\lambda 1909$	75.0	4.3	2.9	1.9	<1.0	<1.0
N II $\lambda 2141$	6.4	<0.4	<0.5	<1.0	<1.0	<1.0
C II] $\lambda 2326$	180	44.0	3.6	2.8	3.5	<1.0	<1.0
[O II] $\lambda 2470$	31	6.5	1.1	0.7	<1.0	<1.0	<1.0
H α $\lambda 6563^a$	1150	165	110	105	62	43	440
H α /H β^a	3.46	5.26	3.65	3.46	3.72	5.42	5.04
$f_\lambda(1300 \text{ \AA})^b$	15	8	4	3	16	7	75
2–10 keV ^c	120	42	13 ± 5^d	29	<3	0.13^d	4 ± 2
β^e	0	–1.5	–0.5	...	–0.5	0	0.5

NOTES.—Except for X-ray fluxes, values are uncorrected for Galactic or internal extinction. Line fluxes in units of $10^{-15} \text{ ergs s}^{-1} \text{ cm}^{-2}$.

^a From Ho et al. 1997a, Stauffer 1982, and Keel 1983.

^b In units of $10^{-16} \text{ ergs s}^{-1} \text{ cm}^{-2} \text{ \AA}^{-1}$.

^c In units of $10^{-13} \text{ ergs s}^{-1} \text{ cm}^{-2}$, after correction for absorption.

^d Extrapolated from *ROSAT* 0.1–2.4 keV data; see text.

^e Spectral slope, $f_\lambda \propto \lambda^\beta$, in the range 1250–2300 Å.

yields a rather implausible $A_{1300} = 9.4$ mag, while the Calzetti et al. curve yields $A_{1300} = 4.4$ mag. In the other four galaxies, the Balmer decrement is in the range 3.4–3.7, implying, after accounting for the Galactic reddening, $A_{1300} = 2.3$ mag from the SMC curve and $A_{1300} = 0.7$ mag using the curve of Calzetti et al.

The two reddening estimators, based on UV slope and on Balmer decrement, are obviously inconsistent, if only because the similar UV slopes of most of the objects suggest similar UV extinction, while the Balmer decrements indicate that some are highly reddened and some are not. A possible solution is that the continuum sources and the line-emitting gas have different dust distribution geometries, with either the gas or the continuum sources undergoing more extinction, depending on the reddening curve assumed. An alternative solution is that different reddening curves operate in the different objects. The two reddening estimators are broadly consistent if the three objects with high Balmer decrements are reddened by the Calzetti et al. curve, while the four objects with low Balmer decrements undergo SMC-like reddening.

3.3. UV Emission Lines and the Ionizing Photon Budget

Except for M81 and NGC 4579, the LINERs have few or no detectable UV emission lines in the G130H range.⁸ Some of them do display emission lines in the mid-UV range, as illustrated in Figure 4. The 1620–2500 Å range (i.e., G190H and part of the G270H range) is plotted with the objects ordered from top to bottom with decreasing equivalent widths of the main lines. Note how the ratio between the two strongest lines, C III] $\lambda 1909$ and C II] $\lambda 2326$, is approximately constant as long as they are detected, while there is a variation by over 2 orders of mag-

nitude in the equivalent width of these lines among the objects. The lines are barely detected in NGC 404 and undetected in NGC 5055 and NGC 4569 despite the high S/N in these three objects. (The emission at 2125 Å in NGC 6500 is an artifact; see Barth et al. 1997.) The UV continuum and the flux in these UV lines are clearly not correlated. This suggests that whatever is generating the UV continuum is not the main driver of the emission lines.

Table 3 lists the mid-UV emission-line fluxes in the seven objects. The fluxes are from a direct integration above a straight-line continuum and for the broad-lined objects include the total (broad- and narrow-line) flux. The Mg II $\lambda 2800$ emission line is not listed, as it is clearly affected to varying degrees by ISM absorption (see, e.g., Fig. 3). Also listed are H α fluxes for each object from Ho et al. (1997a), Stauffer (1982; NGC 5055), and Keel (1983; NGC 4569). For NGC 404, 4569, and 4579, we have verified the photometric accuracy of the nuclear H α flux using narrowband *HST* WFPC2 images, to be described elsewhere. The fluxes listed in Table 3 have not been corrected for Galactic or internal extinction, but in our analysis we use fluxes corrected for Galactic extinction according to the values listed in Table 1.

The conclusion that the UV continua and emission lines are uncorrelated is initially surprising, since it was noted in Maoz et al. (1995) that the H α fluxes of the UV-bright LINERs in their sample are well correlated with the 2200 Å continuum and that the extrapolation of the observed continuum flux (assuming a power law with $\beta = -1$) could provide sufficient ionizing photons to drive the observed H α flux. To reexamine this, we plot in Figure 5 the H α flux versus $f_\lambda(1300 \text{ \AA})$ measured from the spectra and corrected for Galactic extinction. There appears to be little relation between these observables. This departure from the results of Maoz et al. (1995) comes about in several ways. The FOS UV fluxes of NGC 404, 4569, and 5055 are consistent with those measured with the FOC. As discussed by Barth et al. (1996b) and above, the FOS measurement of NGC 4579 is lower than the FOC measurement by a factor of 3. One may

⁸ Fig. 1 of Barth et al. (1997) shows that Ly α is resolved from geocoronal emission in the spectrum of NGC 6500. Also, the extremely weak emission line at 1240 Å, if real, may be Mg II $\lambda\lambda 1239.92, 1240.40$ rather than N V (G. Wallerstein 1998, private communication).

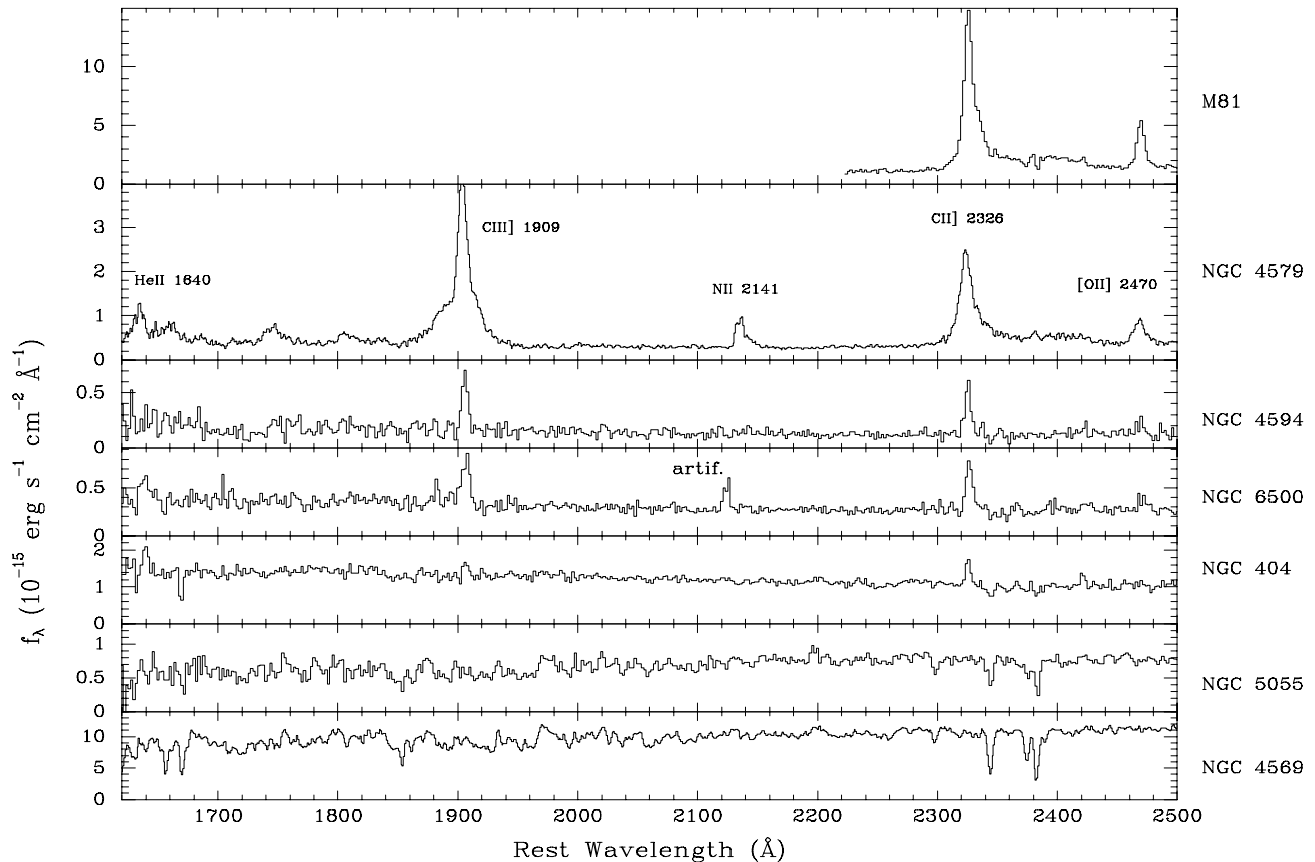


FIG. 4.—FOS spectra of the seven LINERs in the 1620–2500 Å range. The objects are ordered from top to bottom with decreasing equivalent width of the main lines, which are labeled in the spectrum of NGC 4579.

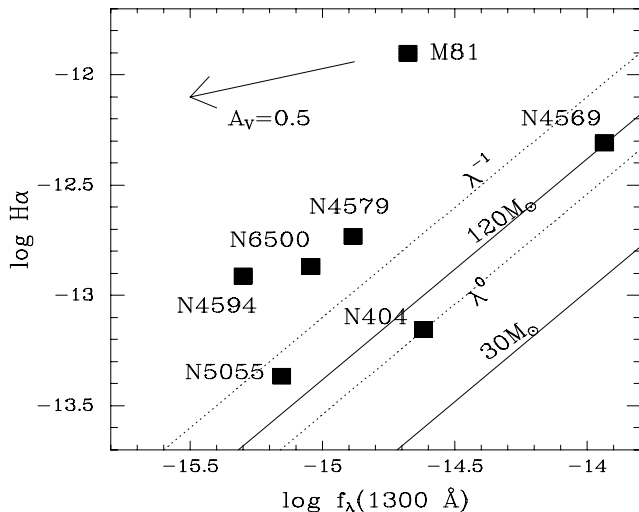


FIG. 5.—Logarithmic H α flux (in $\text{ergs s}^{-1} \text{cm}^{-2}$) vs. $\log f_{\lambda}(1300 \text{ \AA})$ (in $\text{ergs s}^{-1} \text{cm}^{-2} \text{\AA}^{-1}$) measured from the spectra and corrected for Galactic extinction. The two solid diagonal lines show the maximum H α flux that can be produced in case B recombination with 100% covering factor from ionization by a stellar population with a given 1300 Å flux, resulting from an instantaneous burst of age 1 Myr, Salpeter initial mass function, and upper mass cutoff of 120 or 30 M_{\odot} . The two dotted lines show this limit for ionization by power-law continua $f_{\lambda} \propto \lambda^{\beta}$ with $\beta = -1$ or $\beta = 0$. An $A_V = 0.5$ mag foreground extinction vector, assuming a Galactic extinction curve, is shown for reference. Typical uncertainties are 10% in $f_{\lambda}(1300 \text{ \AA})$ (± 0.04 in the log) and 30% in H α flux (about ± 0.13 in the log).

argue that the NGC 4579 point in Figure 5 should be plotted at the FOC position [i.e., $\log f_{\lambda}(1300 \text{ \AA}) = -14.4$, assuming the $f_{\lambda}(1300 \text{ \AA})/f_{\lambda}(2200 \text{ \AA})$ ratio stays constant and correcting for Galactic extinction), either because the FOS measurement is less robust or because the high flux is the “normal” one, which the recombining gas “remembers.” NGC 4594, M81, and NGC 6500 were not in the Maoz et al. (1995) FOC survey, and they ruin the correlation that was suggested by Maoz et al. (1995). As we will show below, all three of these LINERs suffer from severe ionizing photon deficits (as already noted by Ho et al. 1996 for M81 and by Nicholson et al. 1998 for NGC 4594). Note that they would *not* have been missed in the FOC survey and classified as “UV-dark”; M87 and NGC 4736 (which were in the FOC survey, but are not in the present sample) have comparable UV brightnesses and were easily detected by the FOC (see Maoz 1996).

The FOS measurements provide us with new input for estimating the ionizing photon budget in these LINERs. First, we can now measure the UV flux at a wavelength closer to the Lyman limit. Second, we can measure the UV continuum slope in the *HST* range directly, instead of assuming a power law with $\beta = -1$. And third, in at least three of the objects, there are unambiguous spectral signatures of a hot stellar population, so we can estimate the ionizing flux based on the expectations from such a population rather than assuming an extrapolated power-law

continuum. As it happens, all three constraints work toward lowering the estimate of the number of ionizing photons, possibly bringing into the photon-deficit regime even those objects for which Maoz et al. (1995) concluded there was no shortage. The FOS 2200 Å fluxes measured for NGC 404, 4579, and 5055 are lower than their estimated FOC fluxes (see Table 1). Except for NGC 4579, all the LINERs have power-law continua that are softer than $\beta = -1$, leading to a lower 1300 or 912 Å flux. For those LINERs whose continua are dominated by hot stars, there will be fewer ionizing photons than from a power law extrapolated beyond the Lyman limit, because hot stars have a substantial absorption at the Lyman edge.

We have computed the ratio of the H α line flux to the 1300 Å continuum flux density for young star clusters containing populations of O-type stars. We carried out our population synthesis calculations using the Geneva stellar evolutionary tracks for stars with solar metallicity (Schaerer et al. 1993). In our models we employ non-LTE model atmospheres for hot ($T \geq 25,000$ K) stars (Pauldrach et al. 1994; A. W. A. Pauldrach 1997, private communication) to compute the cluster Lyman continuum fluxes. The 1300 Å fluxes are computed with the assumption that the stars radiate as blackbodies at wavelengths longward of the Lyman limit. Further details of these and related computations are described by Tacconi-Garman, Sternberg, & Eckart (1996) and Sternberg (1998). Here we consider young clusters ($\lesssim 10^6$ yr) with Salpeter initial mass functions (IMFs). Assuming case B recombination in 10^4 K ionization-bounded nebulae, the H α line luminosities per number of O-type stars are equal to 1.4×10^{36} and 1.4×10^{37} ergs s $^{-1}$ for IMFs that extend up to 30 and 120 M_{\odot} , respectively. For such clusters the H α / $f_{\lambda}(1300 \text{ Å})$ ratios equal about 10.5 and 42.0 Å, respectively, and decrease with increasing cluster age.

The stellar wind signatures in several of the LINERs require the presence of stars of mass $\gtrsim 30 M_{\odot}$. The two solid lines in Figure 5 show the maximum H α flux that can be produced with 100% covering factor from ionization by a stellar population with the given 1300 Å flux and upper mass cutoff of 120 or 30 M_{\odot} . The two dotted lines show this limit for ionization by power-law continua of the form λ^{β} with $\beta = -1$ or $\beta = 0$.

We see that if there is no internal extinction, then some and possibly all of the LINERs require an additional ionizing source to drive their line flux. M81, NGC 4594, and NGC 6500, even if their UV spectra are extrapolated as power laws with $\beta = -1$ (i.e., harder than observed) rather than as stellar population spectra, also have a severe ionizing photon deficit. NGC 4579, on the other hand, does have a $\beta \approx -1$ slope, as was assumed by Maoz et al. (1995). If the Maoz et al. (1995) flux level is adopted, then, as before, it has a factor of 2.8 ionizing photon surplus, rather than a deficit. If, however, stars dominate the UV continuum or the FOS flux level is the “normal” level, then this LINER also has an ionizing photon deficit. In the three LINERs whose UV emission is clearly dominated by stars (NGC 404, 4569, and 5055), ionization by the stellar population can provide the required power, but only if very massive stars are still present. Interestingly, it is these three objects that also have the lowest emission-line ratios of [O III] $\lambda 5007$ /H β , [O I] $\lambda 6300$ /H α , and [S II] $\lambda 6716$, 6731/H α in the sample (see Ho et al. 1997a); this is exactly what one would expect from ionization by the relatively soft contin-

uum of a significant stellar component, which produces less heating per ionization and a smaller partially ionized zone than does an AGN-like power-law continuum. Stellar photoionization models for LINERs have been presented by Filippenko & Terlevich (1992) and Shields (1992).

Alternatively, some internal foreground extinction (such that the UV emission is attenuated as seen by the observer, but not as seen by the ionized gas) could, in principle, alleviate the ionization budget problem in some of the objects. As discussed in § 3.2 above, the uncertainty in the extinction curve and the many possible configurations for different extinction of the continuum and nebular emission result in a broad range of possible extinction corrections. To illustrate the effect of a plausible extinction correction, Figure 5 shows an $A_V = 0.5$ mag foreground extinction vector, assuming a Galactic extinction curve. A Galactic curve is intermediate in “grayness” between the SMC and Calzetti et al. (1994) curves considered in § 3.2. Note that the objects with the most severe ionizing photon deficits (M81, NGC 4594, and NGC 6500) are those whose Balmer decrements (see Table 3) indicate little internal reddening, $A_V = 0.1$ –0.35 mag, for the range in extinction curves. In NGC 4569, 5055, and 4579, as discussed in § 3.2, a plausible extinction correction will increase in the intrinsic 1300 Å flux by a factor of $\gtrsim 10$ (with a corresponding increase in the number of O-type stars) and may relieve the need for the most massive ($\sim 120 M_{\odot}$) stars.

We conclude that at least some of the LINERs in our sample have an ionizing photon deficit, indicating an additional energy source, beyond that implied by the observable UV. To search for evidence of such an additional source we have compiled X-ray data for the seven LINERs. For NGC 404, 4569, 4579, and 4594, we have used analysis of both archival and new *ASCA* data by Y. Terashima, A. Ptak, and L. Ho (to be described elsewhere) to obtain unabsorbed 2–10 keV fluxes. For M81 we have used the *ASCA* flux derived by Ishisaki et al. (1996). NGC 5055 and NGC 6500 have not been observed with *ASCA*, but they have been observed by *ROSAT* in the 0.1–2.4 keV band. We use the *ROSAT* HRI flux derived by Barth et al. (1997) for NGC 6500 and extrapolate it to the *ASCA* bandpass, assuming an X-ray flux density $f_{\nu} \propto \nu^{-0.7}$. Read, Ponman, & Strickland (1997) have observed NGC 5055 with the *ROSAT* PSPC and find that the nuclear source is best fit with a cool (0.74 keV) thermal plasma, absorbed by a hydrogen column of 2.55×10^{20} cm $^{-2}$, and a flux of 3.3×10^{-13} ergs s $^{-1}$ cm $^{-2}$ escaping from the galaxy. We extrapolate this model to find the unabsorbed 2–10 keV band flux. We caution that the extrapolated fluxes for these two galaxies are uncertain. In the case of NGC 6500, both the instrument (HRI) and the low count statistics preclude any spectral information. In NGC 5055, it is possible that there is a power-law component that dominates over the thermal component in the 2–10 keV band. Table 3 lists our assumed 2–10 keV fluxes for the seven LINERs.

Figure 6 shows the ratio of X-ray to UV power versus H α to UV power for each of the LINERs. Note how in the four “UV photon-starved” objects (high H α -to-UV power ratio) the X-ray power is comparable to or greater than the UV power. Conversely, in the three objects without a serious ionizing photon deficit, the X-ray power is 1 to 2 orders of magnitude lower than the UV power. This suggests that, indeed, an energy source emitting primarily in the extreme-UV, and not directly related to the observed

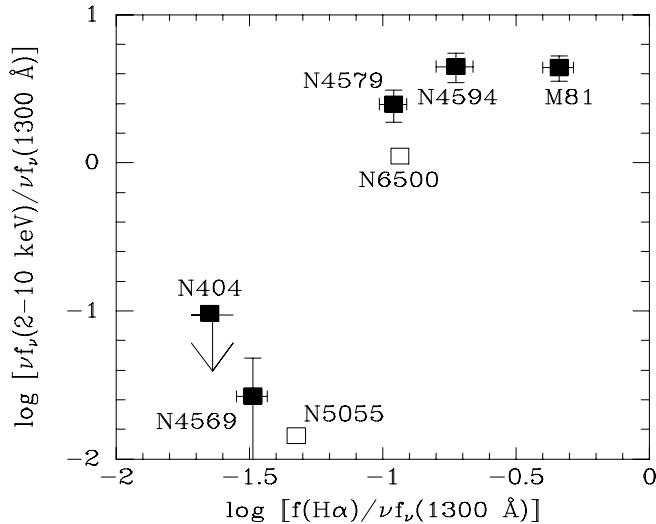


FIG. 6.—Ratio of X-ray to UV power vs. that of H α to UV power for each of the LINERs. Filled symbols denote *ASCA* measurements; open symbols are extrapolated *ROSAT* values. Note how in the four “UV photon-starved” objects (high H α -to-UV power ratio) the X-ray power is comparable to, or greater than, the UV power. An energy source emitting primarily in X-rays, and not necessarily related to the observed UV source, is probably the main ionizing agent in these four objects.

UV source, may be the main ionizing agent in the four UV photon-starved objects. The observed X-ray emission would be the high-energy tail of such a component. For example, a blackbody with temperature greater than 3.3×10^5 K would have an X-ray-to-UV power ratio greater than or equal to that of the UV photon-starved objects. Alternatively, the photoionizing continua in these objects could consist of power-law spectra extending from the X-rays to the Lyman limit. However, this would require that the central UV sources be significantly attenuated by dust extinction while the nebular components are not.

3.4. Ionization Mechanism

It has long been debated whether the emission lines in LINERs are produced by means of photoionization or by shocks. The question has been recently readdressed in the analysis of the four LINERs among the seven discussed here with published UV spectra (Ho et al. 1996; Barth et al. 1996b, 1997; Nicholson et al. 1998). These studies show that the UV line ratios are consistent with either photoionization by an AGN-like continuum or by slow-moving shocks, but inconsistent with the fast “photoionizing” shocks proposed by Dopita & Sutherland (1996).

The three additional LINERs introduced in the present study have either very weak (NGC 404) or undetected (NGC 4569, NGC 5055) UV line emission. For this reason, we chose not to carry out detailed modeling of these three objects. In principle, one could study the ratios, or the lower limits of the ratios, between optical and UV emission lines. However, such ratios are extremely sensitive to the assumed extinction corrections, especially in NGC 4569 and NGC 5055, which have moderately steep Balmer decrements (see Table 3 and discussion in § 3.2). The uncertainty in the magnitude and form of the extinction makes it difficult to exclude any models based on optical-to-UV line ratios.

We note that the ratios of the weak UV lines measured in NGC 404 are similar to those of the previously studied LINERs, so the conclusion regarding the viability of photoionization and slow-moving shocks holds for this object as well. In NGC 4569 and NGC 5055, the complete absence of UV emission lines argues against shock-excitation, since a rich UV emission-line spectrum would be expected given the observed optical line spectrum. Furthermore, the absorption lines in the spectra of these objects show that massive stars exist in the nuclei. The sources required to produce most or all of the emission lines by photoionization are therefore present.

4. CONCLUSIONS

We have studied the *HST* UV spectra of seven LINERs that have compact nuclear UV sources. Our main findings are as follows:

1. At least three of the LINERs have clear spectral signatures indicating that the dominant UV continuum source is a cluster of massive stars.
2. A similar continuum source could dominate in the other four LINERs as well, but its spectral signatures would be veiled by low S/N or superposed broad emission lines. Alternatively, there may be two types of UV-bright LINERs: those in which the UV continuum is produced by a starburst, and those in which it is nonstellar. If the variability of NGC 4579 is real, its continuum source is certainly an AGN.
3. The seven LINERs have similar UV SEDs, which are approximately flat in f_λ . The equivalent widths of the UV emission lines span 2 orders of magnitude. In the objects with the highest S/N, the continuum shape, the UV interstellar absorption lines, the optical line ratios, and the X-ray-absorbing column are all broadly consistent with a starburst spectrum extinguished by $A_V \approx 0.5$ mag.
4. The three “clearly stellar” LINERs have relatively weak X-ray emission, and their stellar populations probably provide enough ionizing photons to explain the observed optical emission-line flux. The four other LINERs have severe ionizing photon deficits, for reasonable extrapolations of their UV spectra beyond the Lyman limit, but an X-ray-to-UV power ratio that is higher by 2 orders of magnitude than that of the three stellar LINERs. A component that emits primarily in the extreme-UV may be the main photoionizing agent in these four objects.

The picture emerging from this comparison is that the compact UV continuum source seen in $\sim 25\%$ of LINERs (Maoz et al. 1995; Barth et al. 1996a, 1998) is, at least in some cases, a nuclear starburst rather than an AGN-like nonstellar object. The UV luminosity is driven by tens to thousands of O-type stars, depending on the object and the extinction assumed. The O stars could be the high-mass end of a bound stellar population, similar to those seen in super-star clusters (e.g., Maoz et al. 1996b).

Nonstellar sources in LINERs may be significant or even dominant at other wavelengths, as we indeed find for some of the objects. Even the three “clearly stellar” LINERs, which do not obviously require the existence of such an additional source, may well have one; the ionizing photon budget estimate was made assuming a 100% covering factor of the line-emitting gas, which is not necessarily true. This picture fits well with recent results showing that nuclear

starburst and quasar-like activity are often intermingled in Seyfert 1 and 2 galaxies. Our results extend this result to the lower luminosities of the LINERs discussed here, although the question of whether a “microquasar” exists in these objects is still open. Apparently, the UV is not the best place to look for microquasars in most LINERs.

Higher S/N UV spectra of some of the objects in our sample could reveal whether they too have the signatures of massive stars. Conversely, further evidence of UV continuum variability, as suggested in NGC 4579, should be sought in LINERs. Even in those LINERs with stellar signatures, UV variability could reveal a contribution by a nonstellar component. Our work suggests, however, that the AGNs possibly associated with LINERs are most prominent at higher energies. X-ray observations by upcoming space missions, having better angular and spec-

tral resolution and higher sensitivity, will likely provide key insights to the nature of LINERs.

We thank A. Ptak and Y. Terashima for generously providing *ASCA* measurements and analysis prior to publication. M. Eracleous and R. Pogge are thanked for permission to use *HST* WFPC2 imaging data and analysis prior to publication. We are grateful to D. Calzetti, T. M. Heckman, A. J. Barth, and an anonymous referee for valuable input. This work was supported by grants GO-6112 and AR-5712 from the Space Telescope Science Institute. NASA grant NAG 5-3556 is also acknowledged. D. M. is grateful for the hospitality of the STScI Visitor Program in the course of this work. D. M. and A. S. acknowledge support from US-Israel Binational Science Foundation grant 94-00300 and by the Israel Science Foundation.

APPENDIX

INTERSTELLAR ABSORPTION LINES IN NGC 4569

The high S/N of the NGC 4569 spectrum reveals numerous interstellar absorption lines. Table 2 lists the strongest detected lines. The spectrum shows narrow absorption features of C I $\lambda\lambda$ 1261, 1277, 1280, 1329, 1561, and 1657 Å, consistent with absorption at the velocity of the galaxy. The equivalent widths of these lines range from 0.5 Å for λ 1280 to 3.5 Å for λ 1657. C I absorption lines in the UV are often present in the spectra of starbursts, but with equivalent widths that are usually less than 1 Å (T. Heckman 1997, private communication). Absorption by C I is noteworthy since its ionization potential is only 11.26 eV; survival of neutral carbon thus requires an environment with substantial shielding or dilution of the radiation at wavelengths longward of the Lyman limit.

UV absorption lines of C I have been observed in Galactic diffuse clouds along several lines of sight (see, e.g., Joseph et al. 1986). The atomic carbon abundance becomes even higher in thicker translucent clouds and at the edges of dense photon-dominated regions, which are hard to observe in UV absorption (because of their high optical depths). Recent work on C I detections in our Galaxy and in starburst galaxies has focused on the two submillimeter fine-structure transitions emitted by the ground-state triplet at 492.2 and 809.3 GHz (see, e.g., Stark & van Dishoeck 1994; Stutzki et al. 1997).

The measured absorption lines can be used to place a bound on the C I column density in NGC 4569. If we assume that absorption occurs on the linear part of the curve of growth, then the resulting values for the column density are inversely correlated with oscillator strength for the six measured transitions, indicating at least partial saturation in the lines. We can then place a conservative lower limit on the column density $N(\text{C I})$ from the transition with the weakest oscillator strength, λ 1280, which implies $N(\text{C I}) \gtrsim 2 \times 10^{15} \text{ cm}^{-2}$. For solar abundances modified by a representative interstellar depletion factor of 0.4 dex (Savage & Sembach 1996), this result implies an accompanying column density of hydrogen $N(\text{H}) \gtrsim 10^{19} \text{ cm}^{-2}$ divided by the carbon neutral fraction.

Similar absorption is also seen in Fe II transitions at 1608, 2344, 2374, 2383, 2587, and 2600 Å, with equivalent widths of ~ 1 –3 Å. These lines also show evidence of saturation and can provide a lower limit on $N(\text{Fe II})$. The velocity structure of the lines indicates a Galactic contribution of roughly a quarter of the total absorption; removing this contribution yields $N(\text{Fe II}) \gtrsim 6 \times 10^{14} \text{ cm}^{-2}$. For solar abundances, the corresponding hydrogen bound is $N(\text{H}) \gtrsim 2 \times 10^{19} \text{ cm}^{-2}$, but this limit would increase to $N(\text{H}) \gtrsim 10^{21} \text{ cm}^{-2}$ for depletion similar to that in the local ISM. Significant absorption ($\gtrsim 0.5$ Å) is *not* detected in the accessible Fe I features, implying $N(\text{Fe I}) \lesssim 2 \times 10^{13} \text{ cm}^{-2}$ and an Fe II/Fe I ionic ratio $\gtrsim 30$.

The H α emission-line flux observed in NGC 4569 suggests that the covering factor of emission-line clouds is high (cf. Fig. 5), and the possibility thus arises that the medium responsible for absorption by C I, Fe II, and other species (Fig. 2) can be identified with such clouds along our line of sight to the continuum source(s). A coherent picture along these lines appears to be possible, with the absorption in NGC 4569 resulting from material with a total column density $N(\text{H I} + \text{H II})$ of a few times 10^{21} cm^{-2} . Standard recombination arguments for ionization-bounded clouds imply that the column density of ionized hydrogen $N(\text{H II})$, expressed in cm^{-2} , scales approximately as $\log N(\text{H II}) = \log U + 23$, where U is the ionization parameter (defined here as the dimensionless ratio of ionizing photon density to particle density at the irradiated cloud face; see Voit 1992). For LINERs, $\log U \approx -3$ to -4 (see, e.g., Ferland & Netzer 1983) so that $N(\text{H II}) \approx 10^{19} - 10^{20} \text{ cm}^{-2}$. This zone will thus constitute an ionized surface on one side of the cloud, with the bulk of the cloud made up of neutral or weakly ionized material. The C I and Fe II column densities, as well as the Fe II/Fe I ratio, will depend on the detailed continuum shape as well as dust shielding, but tests with the photoionization code CLOUDY (Ferland 1996) suggest that the measured bounds are easily plausible in this model, assuming solar abundances and standard depletion factors.

An absorbing column density of this type should have measurable effects on the continuum. Dust associated with the absorbing gas will produce extinction of order $A_V \approx 1$ mag, as is indeed suggested in this galaxy (see § 3.2). The absorbing medium will also imprint bound-free absorption on the soft X-ray emission from NGC 4569. Preliminary fits to *ASCA* spectra of this object suggest that substantial absorption is, in fact, present, with a total hydrogen column density (assuming solar

abundances) of order 10^{22} cm^{-2} (Y. Terashima 1998, private communication), which is in plausible agreement with this picture.

REFERENCES

- Barth, A. J., Ho, L. C., Filippenko, A. V., & Sargent, W. L. W. 1996a, in ASP Conf. Ser. 103, *The Physics of LINERs in View of Recent Observations*, ed. M. Eracleous, A. Koratkar, C. Leitherer, & L. Ho (San Francisco: ASP), 153
- , 1998, *ApJ*, 496, 133
- Barth, A. J., Reichert, G. A., Filippenko, A. V., Ho, L. C., Shields, J. C., Mushotzky, R. F., & Puchnarewicz, E. M. 1996b, *AJ*, 112, 1829
- Barth, A. J., Reichert, G. A., Ho, L. C., Shields, J. C., Filippenko, A. V., & Puchnarewicz, E. M. 1997, *AJ*, 114, 2313
- Bouchet, P., Lequeux, J., Maurice, E., Prévot, L., & Prévot-Burnichon, M. L. 1985, *A&A*, 149, 330
- Burstein, D., & Heiles, C. 1984, *ApJS*, 54, 33
- Calzetti, D. 1997a, *AJ*, 113, 162
- , 1997b, in AIP Conf. Proc. 408, *The Ultraviolet Universe at Low and High Redshift*, ed. W. H. Waller (New York: AIP), 403
- Calzetti, D., Kinney, A. L., & Storchi-Bergmann, T. 1994, *ApJ*, 429, 582
- , 1996, *ApJ*, 458, 132
- Cardelli, J. A., Clayton, G. C., & Mathis, J. S. 1989, *ApJ*, 345, 245
- Conti, P. S., Leitherer, C., & Vacca, W. D. 1996, *ApJ*, 461, L87
- Crane, P., et al. 1993, *AJ*, 106, 1371
- Devereux, N., Ford, H., & Jacoby, G. 1997, *ApJ*, 481, L71
- Dey, A., van Breugel, W., Vacca, W. D., & Antonucci, R. 1997, *ApJ*, 490, 698
- Dopita, M. A., & Sutherland, R. S. 1996, *ApJS*, 102, 161
- Eracleous, M., Koratkar, A., Leitherer, C., & Ho, L., eds. 1996, ASP Conf. Ser. 103, *The Physics of LINERs in View of Recent Observations* (San Francisco: ASP)
- Ferland, G. J. 1996, *HAZY*, a Brief Introduction to Cloudy (Univ. Kentucky Phys. Astron. Dept. Internal Rep.)
- Ferland, G. J., & Netzer, H. 1983, *ApJ*, 264, 105
- Filippenko, A. V., & Sargent, W. L. W. 1985, *ApJS*, 57, 503
- , 1988, *ApJ*, 324, 134
- Filippenko, A. V., & Terlevich, R. 1992, *ApJ*, 397, L79
- Genzel, R., Weitzel, L., Tacconi-Garman, L. E., Blietz, M., Cameron, M., Krabbe, A., Lutz, D., & Sternberg, A. 1995, *ApJ*, 444, 129
- Heckman, T. M. 1980, *A&A*, 87, 152
- , 1998, in *The Most Distant Radio Galaxies*, ed. P. Best, H. Röttgering, & M. Lehnert (Dordrecht: Reidel), in press
- Heckman, T. M., et al. 1997, *ApJ*, 482, 114
- Heckman, T. M., & Leitherer, C. 1997, *AJ*, 114, 69
- Ho, L. C., Filippenko, A. V., & Sargent, W. L. W. 1996, *ApJ*, 462, 183
- , 1997a, *ApJS*, 112, 315
- Ho, L. C., Filippenko, A. V., Sargent, W. L. W., & Peng, C. Y. 1997b, *ApJS*, 112, 391
- Ishisaki, Y., et al. 1996, *PASJ*, 48, 237
- Joseph, C. L., Snow, T. P., Jr., Seab, C. G., & Crutcher, R. M. 1986, *ApJ*, 309, 771
- Keel, W. C. 1983, *ApJ*, 269, 466
- Keel, W. C. 1996, *PASP*, 108, 917
- Kinney, A. L., Calzetti, D., Bohlin, R. C., McQuade, K., Storchi-Bergmann, T., & Schmitt, H. R. 1996, *ApJ*, 467, 38
- Leitherer, C., & Heckman, T. M. 1995, *ApJS*, 96, 9
- Leitherer, C., Robert, C., & Heckman, T. M. 1995, *ApJS*, 99, 173
- Leitherer, C., Vacca, W. D., Conti, P. S., Filippenko, A. V., Robert, C., & Sargent, W. L. W. 1996, *ApJ*, 465, 717
- Lowenthal, J. D., et al. 1997, *ApJ*, 481, 673
- Maoz, D. 1996, in ASP Conf. Ser. 102, *The Physics of LINERs in View of Recent Observations*, ed. M. Eracleous, A. Koratkar, C. Leitherer, & L. Ho (San Francisco: ASP), 90
- Maoz, D., Barth, A. J., Sternberg, A., Filippenko, A. V., Ho, L. C., Macchetto, F. D., Rix, H.-W., & Schneider, D. P. 1996b, *AJ*, 111, 2248
- Maoz, D., Filippenko, A. V., Ho, L. C., Macchetto, F. D., Rix, H.-W., & Schneider, D. P. 1996a, *ApJS*, 107, 215
- Maoz, D., Filippenko, A. V., Ho, L. C., Rix, H.-W., Bahcall, J. N., Schneider, D. P., & Macchetto, F. D. 1995, *ApJ*, 440, 91
- Meurer, G. R., Heckman, T. M., Leitherer, C., Kinney, A., Robert, C., & Garnett, D. R. 1995, *AJ*, 110, 2665
- Murphy, E. M., Lockman, F. J., Laor, A., & Elvis, M. 1996, *ApJS*, 105, 369
- Nicholson, K. L., Reichert, G. A., Mason, K. O., Puchnarewicz, E. M., Ho, L. C., Shields, J. C., & Filippenko, A. V. 1998, *MNRAS*, in press
- Pauldrach, A. W. A., Kudritzki, R.-P., Puls, J., Butler, K., & Hunsinger, J. 1994, *A&A*, 283, 525
- Pei, Y. C. 1992, *ApJ*, 395, 130
- Pettini, M., Kellogg, M., Steidel, C. S., Dickinson, M., Adelberger, K. L., & Giavalisco, M. 1998, *ApJ*, submitted
- Phillips, M. M. 1993, *ApJ*, 413, L105
- Read, A. M., Ponman, T. J., & Strickland, D. K. 1997, *MNRAS*, 286, 626
- Rood, H. J., & Williams, B. A. 1993, *MNRAS*, 263, 211
- Savage, B. D., et al. 1993, *ApJ*, 413, 116
- Savage, B. D., & Sembach, K. R. 1996, *ARA&A*, 34, 279
- Schaerer, D., Meynet, G., Maeder, A., & Schaller, G. 1993, *A&A*, 98, 523
- Shields, J. C. 1992, *ApJ*, 399, L27
- Shields, J. C., & Filippenko, A. V. 1990, *AJ*, 100, 1034
- Stark, R., & van Dishoeck, E. F. 1994, *A&A*, 286, L43
- Stauffer, J. R. 1982, *ApJ*, 262, 66
- Steidel, C. C., Giavalisco, M., Dickinson, M., & Adelberger, K. L. 1996, *AJ*, 112, 352
- Sternberg, A. 1998, *ApJ*, submitted
- Stutzki, J., et al. 1997, *ApJ*, 477, L33
- Tacconi-Garman, L. E., Sternberg, A., & Eckart, A. 1996, *AJ*, 112, 918
- Thatte, N., Quirrenbach, A., Genzel, R., Maiolino, R., & Tecza, M. 1997, *ApJ*, 490, 238
- Tully, R. B. 1988, *Nearby Galaxies Catalog* (Cambridge: Cambridge Univ. Press)
- Vacca, W. D., Robert, C., Leitherer, C., & Conti, P. S. 1995, *ApJ*, 444, 647
- Voit, G. M. 1992, *ApJ*, 399, 495